

Learning Semantic Facial Descriptors for Accurate Face Animation

Lei Zhu¹, Yuanqi Chen¹, Xiaohang Liu¹, Thomas H.Li¹, Ge Li^{1†}

¹*School of Electronic and Computer Engineering, Shenzhen Graduate School, Peking University*

Abstract—Face animation is a challenging task. Existing model-based methods (utilizing 3DMMs or landmarks) often result in a model-like reconstruction effect, which doesn’t effectively preserve identity. Conversely, model-free approaches face challenges in attaining a decoupled and semantically rich feature space, thereby making accurate motion transfer difficult to achieve. We introduce the semantic facial descriptors in learnable disentangled vector space to address the dilemma. The approach involves decoupling the facial space into identity and motion subspaces while endowing each of them with semantics by learning complete orthogonal basis vectors. We obtain basis vector coefficients by employing an encoder on the source and driving faces, leading to effective facial descriptors in the identity and motion subspaces. Ultimately, these descriptors can be recombined as latent codes to animate faces. Our approach successfully addresses the issue of model-based methods’ limitations in high-fidelity identity and the challenges faced by model-free methods in accurate motion transfer. Extensive experiments are conducted on three challenging benchmarks (i.e. VoxCeleb, HDTF, CelebV). Comprehensive quantitative and qualitative results demonstrate that our model outperforms SOTA methods with superior identity preservation and motion transfer.

Index Terms—Face animation, orthogonal basis vector.

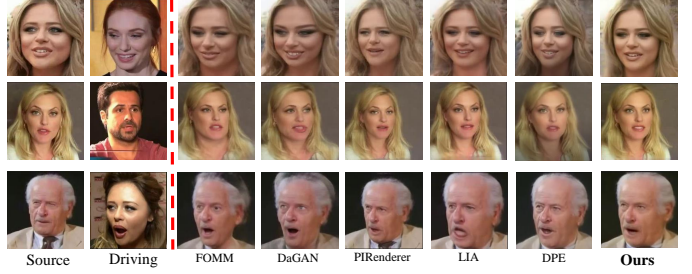
I. INTRODUCTION

Due to the remarkable progress of deep generative models, face animation has drawn increased attention, where the goal is to transfer the motion (3D head orientation and expression) of a target face to a source. Such capabilities give rise to numerous applications, including virtual reality and film production. However, it’s challenging to achieve accuracy in both aspects simultaneously: accurately preserving source identity and transferring target motion.

Many model-based methods [?], [10]–[12], [38], [42], [44], [46], [58]–[61], [72], [75] leverage 3DMMs [40], [62] or landmark detectors [44], [63] to obtain disentangled facial parameters or landmarks containing motion information. 3DMM [40] is built from a large corpus of 3D face scans, using PCA bases to derive a parametric model of facial shape and texture variation. However, the coarse face shapes generated through the computer graphics techniques used in 3DMMs have limited ability to represent the full range of real face shape variations, leading to model-like and not highly realistic results. A limitation of landmark-based methods [37], [44], [46] is that landmarks preserve identity, thus impeding their applicability to cross-id face animation. In addition, using pretrained models can easily lead to error accumulation, especially when the training data for face animation differs from the distribution of pretrained models. Furthermore, using pretrained models suffers from a tedious big-budget construction procedure.

Model-free methods [16], [64], [65], [76] learn to reconstruct driving frames by warping source images utilizing predicted dense flow fields alongside learned explicit facial structural features like landmarks [16], [65] or regions [64]. Nevertheless, these methods struggle to achieve accurate motion transfer and generate numerous artifacts. The reason is that they have difficulty obtaining a highly disentangled feature space that is semantically meaningful. They

(a). Cross-reenactment on the VoxCeleb dataset



(b). Cross-reenactment on the HDTF dataset.

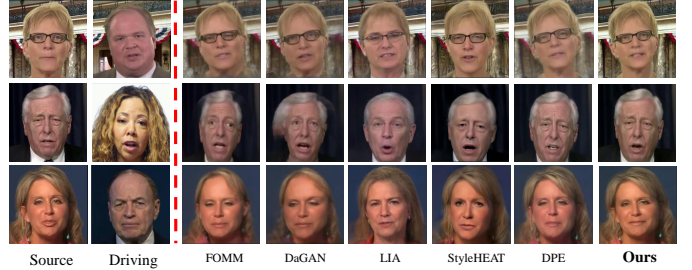


Fig. 1. Qualitative comparisons with SOTA methods on Cross-reenactment.

also have difficulty establishing high-resolution flow fields, limiting applicability to high-resolution animation. Despite [70] employing attention mechanisms for texture completion, such methodologies still encounter challenges in maintaining the fidelity of the identities in the source image.

Unlike these model-based or model-free methods that use explicit structural information, we obtain a face representation that is highly disentangled and semantically meaningful in identity and motion. Our approach effectively addresses the issue of model-based methods’ limitations in achieving high fidelity, and the challenge faced by model-free methods in accurately realizing motion transfer. Inspired by 3DMM’s use of PCA bases to build a parametric model of facial shapes, we wondered: *Can we learn a complete set of orthogonal basis vectors to construct high-level disentangled and semantically meaningful face representations with high fidelity?*

Based on this problem, we learn a highly disentangled vector space in a self-supervised manner and build high-level semantic face descriptors for face animation. According to the requirement of disentangling identity and motion, we assume the face feature space is composed of an identity subspace and a motion subspace, each spanned by a set of complete orthogonal basis vectors. We devise a series of learning strategies to update the vectors so that the two subspaces are decoupled from each other while retaining semantic. We can subsequently perform distinct linear combinations on these basis vectors within the subspaces. The weights of basis vectors encoding specific identities and motions are obtained by effectively extracting information from the source and driving images using encoders, which are optimized during network training. Finally, we combine the identity and motion descriptors from the two subspaces

[†]Corresponding Author

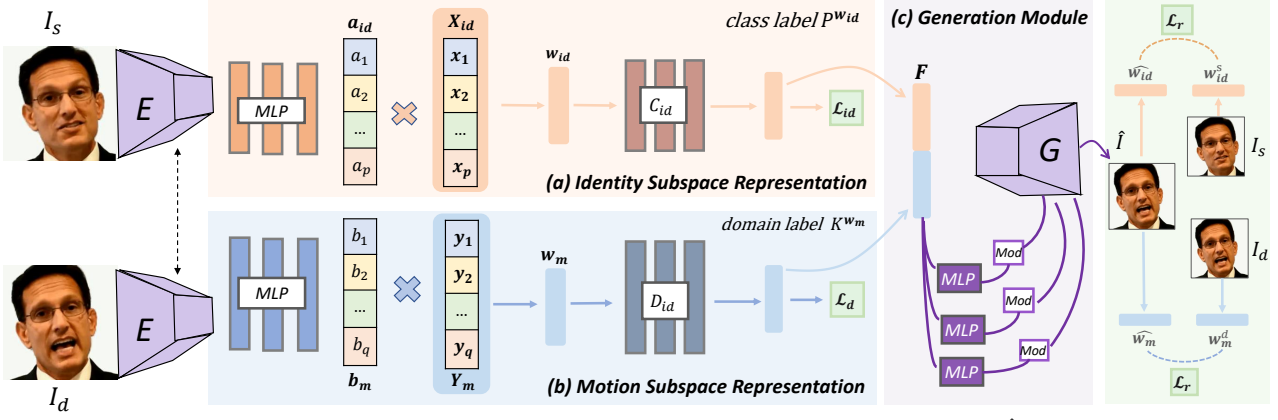


Fig. 2. The pipeline of our method. We take source image I_s and driving image I_d as input and output animated image \hat{I} . Refer to II for the specific process.

as latent codes to control the generation process. We can obtain a series of intermediate states between two motions by simply adjusting the coefficients.

We train from scratch on datasets of two different resolutions (i.e. VoxCeleb, HDTF) and achieve high-fidelity animation results on three test datasets with precise motion transfer. Experiments demonstrate our results far surpass other SOTA methods on wild-face images. The characteristics of our method are summarized as follows:

- High-fidelity: Due to independence from patterned structural information and highly decoupled identity descriptors, we can achieve superior fidelity in identity compared to SOTA model-based approaches.
- High-precise: The motion descriptors possess abundant semantic information, enabling us to achieve more accurate motion transfer compared to SOTA model-free approaches.
- High-efficiency: The space we have constructed is linear, enabling straightforward linear interpolation between two motions. We require no reliance on pretrained models, leading to efficient inference. Additionally, the space we have constructed can be successfully extended to high-resolution image animations.

II. METHOD

A. Face Representation Space

The framework of our proposed method is shown in Fig.2. Instead of using an explicit 3D graphics model, we directly represent human faces in a high-dimensional vector space for 2D face animation. We treat human faces as signals in the physical world. Based on the theory of signal processing, all signals in a vector space can be represented by a complete set of orthogonal basis vectors. Inspired by this characteristic, our idea is to learn a set of orthogonal basis vectors $\mathbf{D} = \{\mathbf{x}_1, \dots, \mathbf{x}_p, \mathbf{y}_1, \dots, \mathbf{y}_q\}$, where a portion of the basis vectors (**identity subspace**) represents identity $\mathbf{X}_{id} = \{\mathbf{x}_1, \dots, \mathbf{x}_p\}$, while the remaining ones capture facial expressions and head poses (**motion subspace**) $\mathbf{Y}_m = \{\mathbf{y}_1, \dots, \mathbf{y}_q\}$. any two basis vectors $\mathbf{d}_i, \mathbf{d}_j \in \mathbf{D}$ follow the constrain

$$\langle \mathbf{d}_i, \mathbf{d}_j \rangle = 0 \text{ if } i \neq j; 1 \text{ if } i = j \quad (1)$$

In our method, we treat \mathbf{D} as a learnable matrix and incorporate the Gram-Schmidt process during each forward pass, ensuring the fulfillment of the orthogonality constraint. We then combine each vector in identity basis with a vector $\mathbf{a}_{id} = \{a_1, \dots, a_p\}$ and in

motion basis with a vector $\mathbf{b}_m = \{b_1, \dots, b_q\}$. Therefore, the face can be modeled as

$$\mathbf{F} = \mathbf{a}_{id}\mathbf{X}_{id} + \mathbf{b}_m\mathbf{Y}_m = \sum_{i=1}^p a_i \mathbf{x}_i + \sum_{i=1}^q b_i \mathbf{y}_i \quad (2)$$

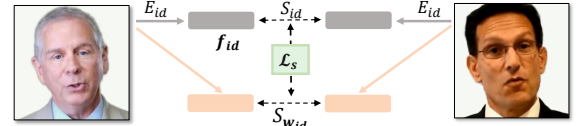


Fig. 3. The pipeline of our identity subspace distillation.

where $\mathbf{x}_i \in \mathbb{R}^N$ and $a_i \in \mathbb{R}$ for all $i \in \{1, \dots, p\}$, $\mathbf{y}_i \in \mathbb{R}^N$ and $b_i \in \mathbb{R}$ for all $i \in \{1, \dots, q\}$. a_i, b_i denotes the weight coefficients of basis vectors corresponding to identity subspace and motion subspace respectively. Supposing that $\mathbf{w}_{id} = \mathbf{a}_{id}\mathbf{X}_{id}$ (**identity subspace descriptor**) corresponds to the identity latent code and $\mathbf{w}_m = \mathbf{b}_m\mathbf{Y}_m$ (**motion subspace descriptor**) corresponds to the motion latent code in the latent space of generation network.

B. Disentangling Identity and Motion Subspaces

To attain complete disentanglement of the identity and motion subspaces, we adopt two mutually reinforcing learning strategies. Firstly, by capitalizing on the feature extraction capabilities of a pretrained facial recognition network, we align the distribution of identity subspace representations with that of true identity features. This allows us to effectively distill identity information in face space. Secondly, we incorporate domain adversarial techniques to eliminate identity-related information from the motion subspaces derived from the driving images.

1) *Identity Subspace Distillation.*: We enhance the identity similarity between images with different motions but the same identity, aiming to incorporate as much identity-related information as possible into the identity subspace representation as shown in Fig.3. By adopting a self-supervised learning strategy, we divide a batch of B samples $\{I_s^1, \dots, I_s^B\}$ into $T = \frac{B}{2}$ pairs $\{(I_s^1, I_s^{T+1}), \dots, (I_s^T, I_s^B)\}$. From this, we obtain T sets of identity subspace representations $\{(\mathbf{w}_{id}^1, \mathbf{w}_{id}^{T+1}), \dots, (\mathbf{w}_{id}^T, \mathbf{w}_{id}^B)\}$ and compute the similarity for each group, resulting in an identity subspace representation similarity vector $\mathbf{s}_{wid} = (s_{wid}^1, \dots, s_{wid}^T)$ of length T . For each binary tuple, we extract identity features using the pre-trained face recognition network ArcFace [32] E_{id} , resulting in T sets of identity features $\{(\mathbf{f}_{id}^1, \mathbf{f}_{id}^{T+1}), \dots, (\mathbf{f}_{id}^T, \mathbf{f}_{id}^B)\}$. We then compute the similarity for each group, yielding a target identity similarity vector $\mathbf{s}_{id} = (s_{id}^1, \dots, s_{id}^T)$ of length T .

The features extracted by the face recognition network provide us with discriminative identity information. By improving the cosine similarity between the identity subspace representation similarity vector $\mathbf{s}_{w_{id}}$ and the target identity similarity vector \mathbf{s}_{id} mentioned above, the identity subspace representation can be made with more discriminative and higher-level identity information. We define the identity similarity loss \mathcal{L}_s as follows.

$$\mathcal{L}_s = -\frac{\mathbf{s}_{id} \cdot \mathbf{s}_{w_{id}}}{\max(\|\mathbf{s}_{id}\|_2 \cdot \|\mathbf{s}_{w_{id}}\|_2, \epsilon)} \quad (3)$$

Where ϵ is a small constant. Finally, we maximize the cosine similarity between the aforementioned two identity similarity vectors.

2) *Eliminating identity in motion subspace.*: In order to ensure that the motion subspace representation does not contain the driving's identity information, we use an identity eraser to eliminate any identity information present in the motion subspace. Specifically, we design a domain discriminator with a 3-layer MLP as the identity eraser. It takes the motion subspace representation \mathbf{w}_m as input and infers its identity domain label as:

$$K^{\mathbf{w}_m} = D_{id}(\mathbf{w}_m) \quad (4)$$

Where $D(\cdot)$ denotes the MLP, $K^{\mathbf{w}_m} \in \mathbb{R}^C$ denotes the predicted identity label, C denotes the number of identities, we optimize the MLP with cross-entropy loss as:

$$\mathcal{L}_d = H(K, K^{\mathbf{w}_m}) \quad (5)$$

Where $H(\cdot)$ denotes cross-entropy loss, and K denotes the one-hot coding of driving's identity label, which is assumed as a vector with the length of identity numbers in the training set. Especially, we use a negative hyperparameter $-\lambda_d$ to introduce the domain loss \mathcal{L}_d as an adversarial loss \mathcal{L}_{adv} into the motion subspace learning to erase any driving's identity. This loss is then used to iteratively optimize both the motion representation generator and the domain discriminator. When the domain discriminator has strong discriminative capabilities, if the loss persists, it can be inferred that identity information in the motion representation has been erased.

C. Enriching Semantic Information in two Subspaces

After separating the two spaces, in order to sufficiently express the semantic in both the identity and motion subspaces, we apply latent regression constraints to the identity subspace and motion subspace, as well as an additional category constraint specifically to enhance identity authentication.

1) *Latent Regression Constraint.*: In order to ensure that the identity of the final generated image \hat{I} remains consistent with the source image I_s and the motion aligns with the driving image I_d , we employ the following latent regression losses \mathcal{L}_r to assist in optimizing two subspaces. This facilitates the sufficient expression of semantic information in both the identity and motion subspaces.

$$\mathcal{L}_r = \|\hat{\mathbf{w}}_{id} - \mathbf{w}_{id}^s\|_1 + \|\hat{\mathbf{w}}_m - \mathbf{w}_m^d\|_1 \quad (6)$$

Where $\hat{\mathbf{w}}_{id}$ and \mathbf{w}_{id}^s respectively denote the identity descriptor extracted from the final generated image \hat{I} and the source image I_s , $\hat{\mathbf{w}}_m$ and \mathbf{w}_m^d respectively denote the motion descriptor extracted from the final generated image \hat{I} and the driving image I_d .

2) *Identity Authentication Enhancement.*: We can further optimize the identity subspace representation \mathbf{w}_{id} through an identity classifier C_{id} using the softmax cross-entropy loss \mathcal{L}_{id} to enhance identity

TABLE I
PERFORMANCE ON VOXCELEB AND CELEBV DATASETS.

	CSIM \uparrow	FID \downarrow	SSIM \uparrow	AED \downarrow	APD \downarrow	CSIM \uparrow	FID \downarrow	SSIM \uparrow	AED \downarrow	APD \downarrow
	VoxCeleb					CelebV				
FOMM	0.480	28.17	0.945	0.149	0.070	0.491	42.30	0.932	0.297	0.105
PIRenderer	0.482	32.60	0.941	0.106	0.069	0.506	41.09	0.940	0.281	0.099
DaGAN	0.466	35.16	0.943	0.135	0.064	0.485	49.99	0.938	0.292	0.093
LIA	0.473	33.58	0.957	0.127	0.066	0.449	52.00	0.941	0.269	0.096
DPE	0.481	31.62	0.957	0.052	0.061	0.476	46.21	0.942	0.266	0.097
Ours	0.503	27.81	0.957	0.035	0.054	0.497	39.46	0.945	0.264	0.092

TABLE II
QUANTITATIVE COMPARISONS ON THE HDTF DATASET.

	CSIM \uparrow	FID \downarrow	SSIM \uparrow	AED \downarrow	APD \downarrow	CSIM \uparrow	FID \downarrow	SSIM \uparrow	AED \downarrow	APD \downarrow
	Self-reenactment					Cross-reenactment				
FOMM	0.712	17.27	0.935	0.113	0.024	0.621	67.74	0.919	0.311	0.049
DaGAN	0.726	24.53	0.917	0.109	0.019	0.594	69.27	0.906	0.302	0.045
LIA	0.320	53.24	0.812	0.271	0.042	0.229	107.34	0.716	0.408	0.051
DPE	0.754	19.87	0.957	0.103	0.019	0.638	54.75	0.938	0.243	0.035
StyleHEAT	0.631	21.61	0.924	0.142	0.031	0.476	62.95	0.915	0.295	0.037
Ours	0.838	18.80	0.969	0.105	0.016	0.724	50.47	0.959	0.269	0.034

authentication. Specifically, the identity classifier produces the probability $P^{\mathbf{w}_{id}} \in \mathbb{R}^C$ that the identity representation belongs to each identity, C denotes the number of identities.

$$\mathcal{L}_{id} = -\log(P_i^{\mathbf{w}_{id}}) \quad (7)$$

where i is the category of the ground-truth identity label.

Once we obtain the face representation $\mathbf{F} = \mathbf{w}_{id} + \mathbf{w}_m$, we take it as our input and use G to decode a flow field $\phi_{s \rightarrow d}$ to warp the source feature $x_s^{enc} = \{x_i^{enc}\}_1^N$ extracted in the encoder E .

D. Training

We train our network in a self-supervised manner to generate \hat{I} using seven losses, i.e., a reconstruction loss \mathcal{L}_{recon} , a perceptual loss \mathcal{L}_{vgg} , an adversarial loss \mathcal{L}_{adv} and four losses mentioned above, i.e., \mathcal{L}_s , \mathcal{L}_d , \mathcal{L}_r , \mathcal{L}_{id} . Our total loss is given by a combination of the aforementioned loss terms:

$$\mathcal{L} = \lambda_{recon} \mathcal{L}_{recon} + \lambda_{vgg} \mathcal{L}_{vgg} + \lambda_{adv} \mathcal{L}_{adv} + \lambda_s \mathcal{L}_s - \lambda_d \mathcal{L}_d + \lambda_r \mathcal{L}_r + \lambda_{id} \mathcal{L}_{id} \quad (8)$$

where we use $\lambda_{recon} = 1$, $\lambda_{vgg} = 1$, $\lambda_{adv} = 1$, $\lambda_s = 2$, $\lambda_d = 0.04$, $\lambda_r = 1$, $\lambda_{id} = 0.05$.

III. EXPERIMENTS

A. Experimental Setup

Dataset We conducted experiments on three public datasets: Vox-Celeb (256-resolution) [27], CelebV [28] (256-resolution) and HDTF [29] (512-resolution). It is noteworthy that all our test sets and their corresponding training sets exhibit no overlap in terms of identities.

Evaluation Metrics For image quality, the Structural Similarity (SSIM) measures the low-level similarity of the generated images to the ground-truth images. The Fréchet Inception Distance (FID) [55] metric is employed to measure the dissimilarity between distributions of generated and real images. Of particular importance, we compute the cosine similarity of identity (CSIM) features to assess the fidelity of identity preservation. These features are derived from the pre-trained face recognition model ArcFace [32]. Furthermore, following the previous work PIRenderer [11], the Average Expression Distance (AED) and Average Pose Distance (APD) metrics are employed to scrutinize the impact of gesture and expression imitation.

Implementation Details The identity and motion subspaces each consist of 20 basis vectors, with 512 dimensions per basis vector.

TABLE III
ABLATION RESULTS OF CROSS-REENACTMENT ON VOXCeleb.

	CSIM \uparrow	FID \downarrow	SSIM \uparrow	AED \downarrow	APD \downarrow
Baseline	0.473	33.58	0.957	0.127	0.066
+Subs.	0.483	32.10	0.957	0.072	0.067
+Dec.	0.498	29.45	0.957	0.053	0.060
+Sem.	0.503	27.81	0.957	0.035	0.054



Fig. 4. Qualitative results of the ablation study. We introduce the identity and motion subspaces (+Subs.), disentangle the two Subspaces (+Dec.) and enrich semantics (+Sem.) in both of them compared to the base model in turn.

B. Quantitative Evaluation

We conducted comparative evaluations between our method and several state-of-the-art (SOTA) approaches: FOMM [16], PIRenderer [11], StyleHEAT [12], DaGAN [33], LIA [66] and DPE [71].

The model trained on the VoxCeleb exhibits quantitative evaluation results for both the VoxCeleb and the CelebV test dataset, as depicted in Tab.I. Our method achieves the best performance among most metrics on VoxCeleb and CelebV on cross-identity facial animation. The significantly improved FID indicates that our image distribution is more similar to the target. The enhanced CSIM score suggests that our approach better preserves the identity of the source image. The exceptional AED and APD values signify that our method achieves more accurate motion transfer. We extended our model to a resolution of 512 and conducted training using the HDTF dataset at this resolution. We performed evaluations on both the same-identity and cross-identity facial animation tasks. The quantitative outcomes of our experimentation are detailed in Tab.II.

C. Qualitative Evaluation

We compare our method with several SOTA methods. The results are displayed in Fig.1. Our approach better preserves source identity and enables smoother motion transfer on VoxCeleb and HDTF dataset, resulting in highly realistic and natural-looking generated images. Although LIA exhibits favorable motion transfer results on low-resolution datasets, its ability to preserve identity remains insufficient. We hypothesize that this phenomenon arises from the fact that the “motion direction vectors” learned by LIA lack explicit semantic information and are coupled with features from the source image. This dual effect adversely affects both the preservation of the source image’s identity and the precision of the learned motion vectors. While DPE yields promising results in expression transfer, the identity and motion are not completely decoupled.

D. Ablation Study

Effectiveness of the various sub-methods. We perform ablation experiments on the VoxCeleb dataset to investigate the effectiveness of the various sub-methods. We add the proposed sub-methods to the base model in turn and report the quantitative results in Tab.III. The improvement in CSIM, AED, and APD demonstrates that the introduction of identity and motion subspaces leads to a noticeable enhancement in preserving identity and facilitating accurate motion

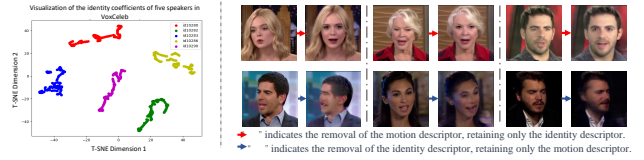


Fig. 5. Visualization for the Subspace Inception Analysis.

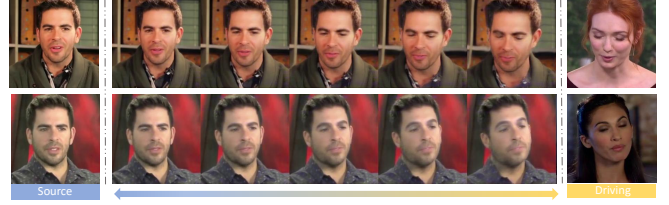


Fig. 6. Interpolation results between 2 speaking styles.

transfer. Upon separating the two subspaces, there is a further advancement in CSIM, as well as AED and APD. Strengthening the semantics in both subspaces enables a comprehensive expression of identity and motion, ultimately achieving high-fidelity identity preservation and precise motion migration. Throughout this process, the FID value consistently improves, indicating increased alignment distribution between the generated image and the target.

The qualitative results are shown in Fig.4. It can be seen that our base model suffers from severe facial distortion, challenges in maintaining identity, and inadequate motion transfer. The introduction of the two subspaces brings a more accurate face shape; however, inaccurate identity representation and imperfect motion emulation persist. By decoupling the two spaces, the generated image’s identity and motion subspaces are isolated from irrelevant information.

E. Subspaces Inspection

Identity Subspace Visualization We project the identity descriptors to a 2D space using t-SNE, which is commonly used in representation learning area [68], [77]–[80]. We select the identity descriptors of 5 different persons from the VoxCeleb test dataset. For each identity, we randomly select 200 frames to extract identity descriptors. In the left of Fig.5, the identity descriptors of the same person cluster in the identity subspace. This implies the identity descriptors of one person are similar. **Distinct Roles of the Two Descriptors** To provide a more intuitive demonstration of the impact of identity and motion descriptors, we randomly selected two sets of photos from the test dataset. For the first set (upper row of the right in Fig.5), we exclusively extracted their identity descriptors while setting the motion descriptors to zero, it is evident that the generated image preserves the original identity and maintains a relatively neutral expression and pose. For the second set (lower row of the right in Fig.5), we extracted their motion descriptors while setting the identity descriptors to zero, it can be observed that the motion descriptor accurately retains motion, while an identity descriptor set to zero signifies that the image loses its facial shape and texture associated with identity.

Motion Manipulation Thanks to the meaningful and linear motion subspace [81]–[83], we can edit the motion by manipulating motion descriptors. As shown in Fig.6, when linearly interpolating between two motion descriptors extracted from different persons, the motion change of generated images transitions smoothly.

IV. CONCLUSION

In this paper, We propose the semantic facial descriptors in learnable disentangled vector space to animate faces. In contrast to

previous works, we successfully address the model-based methods' limitations in high-fidelity identity, and the challenge faced by model-free methods in accurate motion transfer. Extensive results demonstrate that our model far outperforms SOTA methods with superior identity preserving and motion transfer.

V. ACKNOWLEDGEMENT

The work is supported by National Science and Technology Major Project (2024ZD01NL00101) and Guangdong Provincial Key Laboratory of Ultra High Definition Immersive Media Technology (Grant No. 2024B1212010006). We thank all reviewers for their valuable comments.

REFERENCES

- [1] H. Abelson, G. J. Sussman, and J. Sussman, *Structure and Interpretation of Computer Programs*. Cambridge, Massachusetts: MIT Press, 1985.
- [2] R. Baumgartner, G. Gottlob, and S. Flesca, "Visual information extraction with Lixto," in *Proceedings of the 27th International Conference on Very Large Databases*. Rome, Italy: Morgan Kaufmann, September 2001, pp. 119–128.
- [3] R. J. Brachman and J. G. Schmolze, "An overview of the KL-ONE knowledge representation system," *Cognitive Science*, vol. 9, no. 2, pp. 171–216, April–June 1985.
- [4] G. Gottlob, "Complexity results for nonmonotonic logics," *Journal of Logic and Computation*, vol. 2, no. 3, pp. 397–425, June 1992.
- [5] G. Gottlob, N. Leone, and F. Scarcello, "Hypertree decompositions and tractable queries," *Journal of Computer and System Sciences*, vol. 64, no. 3, pp. 579–627, May 2002.
- [6] H. J. Levesque, "Foundations of a functional approach to knowledge representation," *Artificial Intelligence*, vol. 23, no. 2, pp. 155–212, July 1984.
- [7] —, "A logic of implicit and explicit belief," in *Proceedings of the Fourth National Conference on Artificial Intelligence*. Austin, Texas: American Association for Artificial Intelligence, August 1984, pp. 198–202.
- [8] B. Nebel, "On the compilability and expressive power of propositional planning formalisms," *Journal of Artificial Intelligence Research*, vol. 12, pp. 271–315, 2000.
- [9] IJCAI Proceedings, "IJCAI camera ready submission," <https://proceedings.ijcai.org/info>.
- [10] Y. Wang, C. Xu, J. Zhu, W. Chu, Y. Tai, C. Wang, J. Li, Y. Wu, F. Huang, and R. Ji, "Hififace: 3d shape and semantic prior guided high fidelity face swapping," *IJCAI*, 2021.
- [11] Y. Ren, G. Li, Y. Chen, T. H. Li, and S. Liu, "Pirenderer: Controllable portrait image generation via semantic neural rendering," in *ICCV*, 2021.
- [12] F. Yin, Y. Zhang, X. Cun, M. Cao, Y. Fan, X. Wang, Q. Bai, B. Wu, J. Wang, and Y. Yang, "Styleheat: One-shot high-resolution editable talking face generation via pre-trained stylegan," in *ECCV*. Springer, 2022.
- [13] M. Meshry, S. Suri, L. S. Davis, and A. Shrivastava, "Learned spatial representations for few-shot talking-head synthesis," *CVPR*, 2021.
- [14] E. Zakharov, A. Ivakhnenko, A. Shysheya, and V. Lempitsky, "Fast bi-layer neural synthesis of one-shot realistic head avatars," *Springer*, 2020.
- [15] A. Siarohin, S. Lathuilière, S. Tulyakov, E. Ricci, and N. Sebe, "Animating arbitrary objects via deep motion transfer," in *CVPR*, 2019.
- [16] —, "First order motion model for image animation," *NeurIPS*, 2019.
- [17] A. Siarohin, O. J. Woodford, J. Ren, M. Chai, and S. Tulyakov, "Motion representations for articulated animation," in *CVPR*, 2021.
- [18] E. Burkov, I. Pasechnik, A. Grigorev, and V. Lempitsky, "Neural head reenactment with latent pose descriptors," in *CVPR*, 2020.
- [19] Y. Nirkin, Y. Keller, and T. Hassner, "Fsgan: Subject agnostic face swapping and reenactment," *CVPR*, 2019.
- [20] E. Zakharov, A. Shysheya, E. Burkov, and V. Lempitsky, "Few-shot adversarial learning of realistic neural talking head models," in *ICCV*, 2019.
- [21] H. Zhang, Y. Ren, Y. Chen, G. Li, and T. H. Li, "Exploiting multiple guidance from 3dmm for face reenactment," in *AAAI Workshop*, 2023.
- [22] Y. Ganin, E. Ustinova, H. Ajakan, P. Germain, H. Larochelle, F. Laviolette, M. Marchand, and V. Lempitsky, "Domain-adversarial training of neural networks," *The journal of machine learning research*, vol. 17, no. 1, 2016.
- [23] Y. Deng, J. Yang, S. Xu, D. Chen, Y. Jia, and X. Tong, "Accurate 3d face reconstruction with weakly-supervised learning: From single image to image set," in *CVPR workshops*, 2019.
- [24] —, "Accurate 3d face reconstruction with weakly-supervised learning: From single image to image set," *Cornell University*, 2019.
- [25] M. Xu, Y. Chen, S. Liu, T. H. Li, and G. Li, "Structure-transformed texture-enhanced network for person image synthesis," in *ICCV*, 2021.
- [26] J. Johnson, A. Alahi, and L. Fei-Fei, "Perceptual losses for real-time style transfer and super-resolution," in *ECCV*, 2016.
- [27] A. Nagrani, J. S. Chung, and A. Zisserman, "Voxceleb: a large-scale speaker identification dataset," *arXiv preprint arXiv:1706.08612*, 2017.
- [28] W. Wu, Y. Zhang, C. Li, C. Qian, and C. C. Loy, "Reenactgan: Learning to reenact faces via boundary transfer," in *ECCV*, 2018.
- [29] Z. Zhang, L. Li, Y. Ding, and C. Fan, "Flow-guided one-shot talking face generation with a high-resolution audio-visual dataset," in *CVPR*, 2021.
- [30] A. Siarohin, S. Lathuilière, S. Tulyakov, E. Ricci, and N. Sebe, "First order motion model for image animation," *NeurIPS*, 2019.
- [31] R. Zhang, P. Isola, A. A. Efros, E. Shechtman, and O. Wang, "The unreasonable effectiveness of deep features as a perceptual metric," in *CVPR*, 2018.
- [32] J. Deng, J. Guo, N. Xue, and S. Zafeiriou, "Arcface: Additive angular margin loss for deep face recognition," in *CVPR*, 2019.
- [33] F.-T. Hong, L. Zhang, L. Shen, and D. Xu, "Depth-aware generative adversarial network for talking head video generation," in *CVPR*, 2022.
- [34] X. Huang and S. Belongie, "Arbitrary style transfer in real-time with adaptive instance normalization," in *ICCV*, 2017.
- [35] M. C. Doukas, S. Zafeiriou, and V. Sharmanska, "Headgan: One-shot neural head synthesis and editing," in *ICCV*, 2021.
- [36] G. Yao, Y. Yuan, T. Shao, and K. Zhou, "Mesh guided one-shot face reenactment using graph convolutional networks," in *ACM MM*, 2020.
- [37] J. Liu, P. Chen, T. Liang, Z. Li, C. Yu, S. Zou, J. Dai, and J. Han, "Li-net: Large-pose identity-preserving face reenactment network," in *ICME*. IEEE, 2021.
- [38] K. Yang, K. Chen, D. Guo, S.-H. Zhang, Y.-C. Guo, and W. Zhang, "Face2face ρ : Real-time high-resolution one-shot face reenactment," in *ECCV*. Springer, 2022.
- [39] J. Liu, W. Li, H. Pei, Y. Wang, F. Qu, Y. Qu, and Y. Chen, "Identity preserving generative adversarial network for cross-domain person re-identification," *IEEE Access*, vol. 7, 2019.
- [40] V. Blanz and T. Vetter, "A morphable model for the synthesis of 3d faces," *SIGGRAPH*, 1999.
- [41] S. Ha, M. Kersner, B. Kim, S. Seo, and D. Kim, "Marionette: Few-shot face reenactment preserving identity of unseen targets," in *AAAI*, vol. 34, no. 07, 2020.
- [42] F. Zhu, J. Zhu, W. Chu, Y. Tai, Z. Xie, X. Huang, and C. Wang, "Hififace: One-shot high fidelity neural head synthesis with 3d control," in *IJCAI*, 2022.
- [43] X. Zhu, C. Yu, D. Huang, Z. Lei, H. Wang, and S. Z. Li, "Beyond 3dmm: Learning to capture high-fidelity 3d face shape," *TPAMI*, vol. 45, no. 2, 2022.
- [44] B. Zhang, C. Qi, P. Zhang, B. Zhang, H. Wu, D. Chen, Q. Chen, Y. Wang, and F. Wen, "Metaportrait: Identity-preserving talking head generation with fast personalized adaptation," in *CVPR*, 2023.
- [45] T.-C. Wang, A. Mallya, and M.-Y. Liu, "One-shot free-view neural talking-head synthesis for video conferencing," in *CVPR*, 2021.
- [46] G.-S. Hsu, C.-H. Tsai, and H.-Y. Wu, "Dual-generator face reenactment," in *CVPR*, 2022.
- [47] X. Chen, Y. Duan, R. Houthoofd, J. Schulman, I. Sutskever, and P. Abbeel, "Infogan: Interpretable representation learning by information maximizing generative adversarial nets," *NeurIPS*, vol. 29, 2016.
- [48] I. Higgins, L. Matthey, A. Pal, C. Burgess, X. Glorot, M. Botvinick, S. Mohamed, and A. Lerchner, "beta-vae: Learning basic visual concepts with a constrained variational framework," in *ICLR*, 2016.
- [49] Y. Wei, Y. Shi, X. Liu, Z. Ji, Y. Gao, Z. Wu, and W. Zuo, "Orthogonal jacobian regularization for unsupervised disentanglement in image generation," in *ICCV*, 2021.
- [50] F. Locatello, S. Bauer, M. Lucic, G. Raetsch, S. Gelly, B. Schölkopf, and O. Bachem, "Challenging common assumptions in the unsupervised learning of disentangled representations," in *ICML*. PMLR, 2019.
- [51] P. Paysan, R. Knothe, B. Amberg, S. Romdhani, and T. Vetter, "A 3d face model for pose and illumination invariant face recognition," in *2009 sixth IEEE international conference on advanced video and signal based surveillance*. Ieee, 2009.

- [52] A. Pumarola, A. Agudo, A. M. Martinez, A. Sanfeliu, and F. Moreno-Noguer, "Ganimation: Anatomically-aware facial animation from a single image," in *ECCV*, 2018.
- [53] C. Donahue, Z. C. Lipton, A. Balsubramani, and J. McAuley, "Semantically decomposing the latent spaces of generative adversarial networks," *arXiv preprint arXiv:1705.07904*, 2017.
- [54] A. Hore and D. Ziou, "Image quality metrics: Psnr vs. ssim," in *2010 20th international conference on pattern recognition*. IEEE, 2010.
- [55] M. Heusel, H. Ramsauer, T. Unterthiner, B. Nessler, and S. Hochreiter, "Gans trained by a two time-scale update rule converge to a local nash equilibrium," *NeurIPS*, vol. 30, 2017.
- [56] A. Paszke, S. Gross, F. Massa, A. Lerer, J. Bradbury, G. Chanan, T. Killeen, Z. Lin, N. Gimelshein, L. Antiga *et al.*, "Pytorch: An imperative style, high-performance deep learning library," *NeurIPS*, vol. 32, 2019.
- [57] D. P. Kingma, "Adam: A method for stochastic optimization/diederik p," *Kingma, Jimmy Ba*, URL: <https://arxiv.org/abs/1412.6980>, 2015.
- [58] G.-S. Hsu, C.-H. Tsai, and H.-Y. Wu, "Dual-generator face reenactment," in *CVPR*, 2022.
- [59] Y. Fan, Z. Lin, J. Saito, W. Wang, and T. Komura, "Faceformer: Speech-driven 3d facial animation with transformers," in *CVPR*, 2022.
- [60] K. Yang, K. Chen, D. Guo, S.-H. Zhang, Y.-C. Guo, and W. Zhang, "Face2face ρ : Real-time high-resolution one-shot face reenactment," in *ECCV*. Springer, 2022.
- [61] M. Agarwal, R. Mukhopadhyay, V. P. Nambodiri, and C. Jawahar, "Audio-visual face reenactment," in *WACV*, 2023.
- [62] P. Paysan, R. Knothe, B. Amberg, S. Romdhani, and T. Vetter, "A 3d face model for pose and illumination invariant face recognition," in *AVSS*. Ieee, 2009.
- [63] E. Wood, T. Baltrušaitis, C. Hewitt, M. Johnson, J. Shen, N. Milosavljević, D. Wilde, S. Garbin, T. Sharp, I. Stojiljković *et al.*, "3d face reconstruction with dense landmarks," in *ECCV*. Springer, 2022.
- [64] A. Siarohin, O. J. Woodford, J. Ren, M. Chai, and S. Tulyakov, "Motion representations for articulated animation," in *CVPR*, 2021.
- [65] T.-C. Wang, A. Mallya, and M.-Y. Liu, "One-shot free-view neural talking-head synthesis for video conferencing," in *CVPR*, 2021.
- [66] Y. Wang, D. Yang, F. Bremond, and A. Dantcheva, "Latent image animator: Learning to animate images via latent space navigation," *arXiv preprint arXiv:2203.09043*, 2022.
- [67] Z. Wang, A. C. Bovik, H. R. Sheikh, and E. P. Simoncelli, "Image quality assessment: from error visibility to structural similarity," *TIP*, vol. 13, no. 4, 2004.
- [68] L. Van der Maaten and G. Hinton, "Visualizing data using t-sne," *Journal of machine learning research*, vol. 9, no. 11, 2008.
- [69] A. Siarohin, O. J. Woodford, J. Ren, M. Chai, and S. Tulyakov, "Motion representations for articulated animation," in *CVPR*, 2021.
- [70] F.-T. Hong and D. Xu, "Implicit identity representation conditioned memory compensation network for talking head video generation," in *Proceedings of the IEEE/CVF International Conference on Computer Vision*, 2023, pp. 23 062–23 072.
- [71] Y. Pang, Y. Zhang, W. Quan, Y. Fan, X. Cun, Y. Shan, and D.-m. Yan, "Dpe: Disentanglement of pose and expression for general video portrait editing," in *Proceedings of the IEEE/CVF Conference on Computer Vision and Pattern Recognition*, 2023, pp. 427–436.
- [72] W. Yu, Y. Fan, Y. Zhang, X. Wang, F. Yin, Y. Bai, Y.-P. Cao, Y. Shan, Y. Wu, Z. Sun *et al.*, "Nofa: Nerf-based one-shot facial avatar reconstruction," in *ACM SIGGRAPH 2023 Conference Proceedings*, 2023, pp. 1–12.
- [73] Z. Ma, X. Zhu, G.-J. Qi, Z. Lei, and L. Zhang, "Otavatar: One-shot talking face avatar with controllable tri-plane rendering," in *Proceedings of the IEEE/CVF Conference on Computer Vision and Pattern Recognition*, 2023, pp. 16 901–16 910.
- [74] Y. Bai, Y. Fan, X. Wang, Y. Zhang, J. Sun, C. Yuan, and Y. Shan, "High-fidelity facial avatar reconstruction from monocular video with generative priors," in *Proceedings of the IEEE/CVF Conference on Computer Vision and Pattern Recognition*, 2023, pp. 4541–4551.
- [75] P. Jin, H. Li, Z. Cheng, K. Li, X. Ji, C. Liu, L. Yuan, and J. Chen, "Diffusionret: Generative text-video retrieval with diffusion model," in *Proceedings of the IEEE/CVF international conference on computer vision*, 2023, pp. 2470–2481.
- [76] H. Li, J. Huang, P. Jin, G. Song, Q. Wu, and J. Chen, "Weakly-supervised 3d spatial reasoning for text-based visual question answering," *IEEE Transactions on Image Processing*, vol. 32, pp. 3367–3382, 2023.
- [77] H. Li, D. Long, L. Yuan, Y. Wang, Y. Tian, X. Wang, and F. Mo, "Decoupled peak property learning for efficient and interpretable electronic circular dichroism spectrum prediction," *Nature Computational Science*, pp. 1–11, 2025.
- [78] H. Li, Y. Jia, P. Jin, Z. Cheng, K. Li, J. Sui, C. Liu, and L. Yuan, "Freestylere: Retrieving images from style-diversified queries," in *European Conference on Computer Vision*. Springer, 2025, pp. 258–274.
- [79] H. Li, P. Jin, Z. Cheng, S. Zhang, K. Chen, Z. Wang, C. Liu, and J. Chen, "Tg-vqa: Ternary game of video question answering," *arXiv preprint arXiv:2305.10049*, 2023.
- [80] H. Li, X. Li, B. Karimi, J. Chen, and M. Sun, "Joint learning of object graph and relation graph for visual question answering," in *2022 IEEE International Conference on Multimedia and Expo (ICME)*. IEEE, 2022, pp. 01–06.
- [81] P. Jin, H. Li, Z. Cheng, K. Li, R. Yu, C. Liu, X. Ji, L. Yuan, and J. Chen, "Local action-guided motion diffusion model for text-to-motion generation," in *European Conference on Computer Vision*. Springer, 2025, pp. 392–409.
- [82] P. Jin, H. Li, L. Yuan, S. Yan, and J. Chen, "Hierarchical banzhaf interaction for general video-language representation learning," *IEEE Transactions on Pattern Analysis and Machine Intelligence*, 2024.
- [83] L. Lv, H. Li, Y. Wang, Z. Yan, Z. Chen, Z. Lin, L. Yuan, and Y. Tian, "Navigating chemical-linguistic sharing space with heterogeneous molecular encoding," *arXiv preprint arXiv:2412.20888*, 2024.